CONSTRAINING THE DEPTH OF POLAR ICE DEPOSITS AND EVOLUTION OF COLD TRAPS ON MERCURY WITH SMALL CRATERS IN PERMANENTLY SHADOWED REGIONS. Ariel N. Deutsch[1], James W. Head[1], Gregory A. Neumann[2], Nancy L. Chabot[3], [1]Department of Earth, Environmental and Planetary Sciences, Brown University, Providence, RI 02912, USA (ariel_deutsch@brown.edu), [2]NASA Goddard Space Flight Center, Greenbelt, MD 20771, USA, [3]The Johns Hopkins University Applied Physics Laboratory, Laurel, MD 20723, USA.

Introduction: Earth-based radar observations revealed highly reflective deposits at the poles of Mercury [e.g., 1], which collocate with permanently shadowed regions (PSRs) detected from both imagery and altimetry by the MErcury Surface, Space ENvironment, GEochemistry, and Ranging (MESSENGER) spacecraft [e.g., 2]. MESSENGER also measured higher hydrogen concentrations at the north polar region, consistent with models for these deposits to be composed primarily of water ice [3].

Enigmatic to the characterization of ice deposits on Mercury is the thickness of these radar-bright features. A current minimum bound of several meters exists from the radar measurements, which show no drop in the radar cross section between 13- and 70-cm wavelength observations [4, 5]. A maximum thickness of 300 m is based on the lack of any statistically significant difference between the height of craters that host radar-bright deposits and those that do not [6]. More recently, this upper limit on the depth of a typical ice deposit has been lowered to ~150 m, in a study that found a mean excess thickness of 50 ± 35 m of radar-bright deposits for 6 craters [7]. Refining such a constraint permits the derivation of a volumetric estimate of the total polar ice on Mercury, thus providing insight into possible sources of water ice on the planet.

Here, we take a different approach to constrain the thickness of water-ice deposits. Permanently shadowed surfaces have been resolved in images acquired with the broadband filter on MESSENGER's wide-angle camera (WAC) using low levels of light scattered by crater walls and other topography [8]. These surfaces are not featureless and often host small craters (< a few km in diameter). Here we utilize the presence of these small simple craters to constrain the thickness of the radar-bright ice deposits on Mercury. Specifically, we compare estimated depths made from depth-to-diameter ratios and depths from individual Mercury Laser Altimeter (MLA) tracks to constrain the fill of material of small craters that lie within the permanently shadowed, radar bright deposits of 7 north polar craters.

Methodology: During its final year of operations, MESSENGER acquired the highest-spatial-resolution views of Mercury's polar deposits, and imaged PSRs within north polar craters [9]. For 7 of these craters, we identify small (< a few km in diameter) craters within the PSRs of the host crater that are bisected by (MLA) tracks. If these small craters pre-dated ice emplacement, then the infilled material can constrain the thickness of the ice within them. We suggest that the small craters were formed before the ice was delivered to these regions because albedo variations are not correlated with the small craters, and there is no evidence for ejecta, although this could be a resolution effect of the images.

Depth-to-diameter ratios. Measurements were taken of the diameters of any craters that are visible in the permanently shadowed, radar-bright deposits. The depth of each small crater was then derived using the defined power function for simple craters on Mercury [10].

There are uncertainties associated with the depth-to-diameter calculations based on the power function [10]. We make our infill estimations from the average power function [10], although assuming a deeper or shallower crater can change the estimated infill by tens of meters. In addition, if these small craters are secondary craters rather than primary craters, then the depth of the crater is overestimated here, and thus the estimated thickness of ice provides a maximum constraint.

Depths from MLA data. The catalogue of small craters within the PSRs of each of the 7 north polar craters was compared to MLA data. We constructed topographic profiles for each of the small craters that was bisected by MLA measurements. Individual MLA altitude measurements have absolute range uncertainties of 1 m [11].

Results: We have identified 10 small craters that are intersected by MLA data (***Table 1***). The craters range in diameter from 0.3 to 4.5 km in diameter, with an average of 1.0 km. These small craters are located within 7 individual, larger north polar craters. From the differences between the expected depth that was derived from depth-to-diameter ratios [10] and the measured depth using MLA data (***Fig. 1***), the average estimated infill of material for 9 of these small identified craters is ~68 ± 25 m. The estimated material infill for these 9 craters ranged from ~25 m in thickness to ~95 m in thickness.

The tenth crater in our dataset has an estimated infill of material of magnitudes larger, approximately 335 m. This anomalous 4.5-km crater is on the margin of the floor of Desprez crater (***Fig. 2***). Because this small crater is located at the base of the wall of Desprez, substantial mass wasting likely contributed additional material to the crater interior. Thus the calculated difference in depths is not likely to be representative of a pure ice thickness, but may include substantial regolith as well.

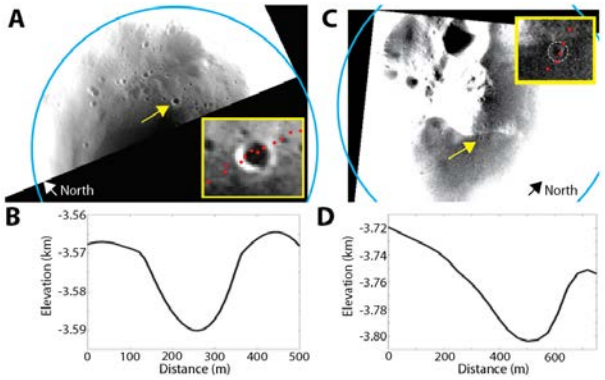

Fig. 1. Results for 2 of the identified 10 small craters. (A) Carolan crater (24 km) centered at 83.9°N, 31.8°E shown in WAC broadband EW1051372081B. Arrow points to small 0.5-km crater, for which topographic profile is shown in (B). Inset shows crater of interest with intersecting MLA pulses (red). (C) An unnamed crater (20 km) centered at 79.5°N, 149.2°E shown in WAC broadband image EW1068970874B. Arrow points to small 0.3-km crater, for which topographic profile is shown in (D). Inset shows crater of interest with intersecting MLA pulses (red).

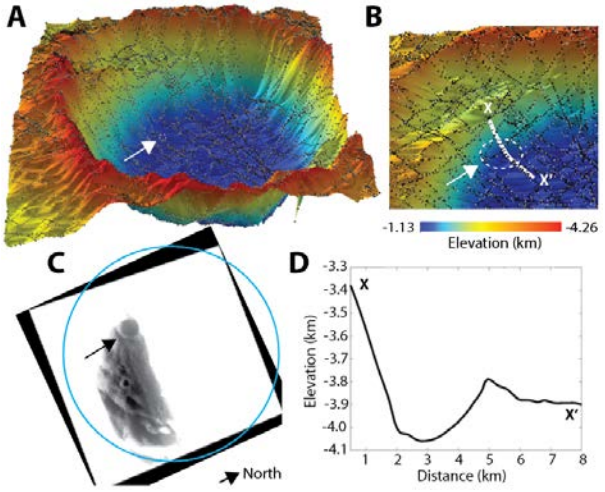

Fig. 2. Desprez crater (47 km) centered at 81.1°N, 258.7°E. Arrow points to small 4.5-km crater studied in (A)–(C). (A) 3-D model of Desprez derived from MLA pulses (shown in black). (B) Expanded view of the small crater of interest. Topographic profile along MLA data delineated in white. (C) WAC image EW1068404967B reveals the crater of interest (arrow). (D) Topographic profile derived from MLA data.

Discussion: If these identified small craters pre-date the deposition of ice, then the infilled material provides a maximum estimate for the amount of water ice within these specific small craters. Other material, however, may contribute to crater infill, including ejecta from more recent impacts or material transported down slope. Complicated crater topographies may also contribute to the difference between the extrapolated depth from depth-to-diameter ratios [10] and the MLA measured depth, given that craters are not perfectly axisymmetric.

Constraining the depth of water-ice deposits on Mercury is critical, given the large range of bounds that currently exist. While the areal distribution of PSRs and radar-bright deposits is well-characterized [2], the thickness of these deposits is not. Such a measurement allows for the volumetric calculation of water-ice deposits on Mercury. Using the areal coverage of radar-bright material [1] and assuming the south pole hosts the same amount of radar-bright material as the north pole, then the total mass of water ice emplaced on Mercury is ~1.4 x 10^{15} kg, if a thickness of 68 ± 25 m is typical for all water-ice deposits on the surface of Mercury. This is consistent with the recent estimates [7].

Such a measurement can provide insight into possible sources based on the flux of water delivered from different mechanisms. Regularly impacting micrometeoroids could deliver water to Mercury, although the modeled impact flux varies between models [12–15]. When using the lower estimates of water delivery [12], our estimated thickness suggests that micrometeorite bombardment alone is not capable of delivering the required amount of water to the poles of Mercury. The higher estimates [13–15], however, lie within the predicted range for water delivery, as do Jupiter-family comets [12]. Given the uncertainties associated with our data, we refrain from ruling out potential sources.

Table 1. Results for craters that are intersected by MLA data.

Host Crater	Lat (°N)	Long (°E)	Depth (m)	Diameter (km)	Estimated Infill (m)
Unnamed	79.4	149.5	77	0.30	25
Unnamed	79.2	82.4	86	0.35	32
Unnamed	80.6	143.8	272	1.8	64
Unnamed	80.5	142.9	126	0.60	73
Carolan	84.1	31.8	100	0.43	77
Ensor	82.4	341.8	109	0.49	83
Fuller	82.5	317.0	95	0.40	84
Ensor	82.3	341.6	118	0.55	94
Carolan	84.0	31.2	118	0.55	95
Desprez	81.0	257.1	516	4.5	336

References: [1] Harmon J. K. et al. (2011) *Icarus, 211,* 37–50. [2] Deutsch A. N. (2016) *Icarus, 280,* 158–171. [3] Lawrence D. J. et al. (2013) *Science, 339,* 292–296. [4] Black G. J. et al. (2010) *Icarus, 209,* 224–229. [5] Harmon J. K. (2007) *Space Sci. Rev., 132,* 307–349. [6] Talpe M. J. et al. (2012) *JGR, 117,* E00L13. [7] Eke V. R. et al. (2017) *Icarus, 284,* 407–415. [8] Chabot N. L. et al. (2014) *Geology, 42,* 1051–1054. [9] Chabot N. L. et al. (2016) *GRL, 43,* 9461–9468. [10] Barnouin O. S. et al. (2012) *Icarus, 219,* 414–427. [11] Zuber M. T. et al. (2012) *Science, 336,* 217–220. [12] Moses J. I. et al. (1999) *Icarus, 137,* 197–221. [13] Bruck Syal et al. (2015) *Nat. Geosci., 8,* 352–356. [14] Nesvorný et a. (2010) *Astrophys., 713,* 816–836. [15] Borin et al. (2009) *A&A, 503,* 259–264.